Title

Human chromosome 21 orthologous region on mouse chromosome 17 is a major determinant of Down syndrome-related developmental cognitive deficits

Journal

Human Molecular Genetics, 23(3)

ISSN

0964-6906

Authors

Zhang, Li
Meng, Kai
Jiang, Xiaoling
et al.

Publication Date

2014-02-01

DOI

10.1093/hmg/ddt446

Peer reviewed

Human Molecular Genetics, 2014, Vol. 23, No. 3 ***578–589***
doi:10.1093/hmg/ddt446
Advance Access published on September 16, 2013

Human chromosome 21 orthologous region on mouse chromosome 17 is a major determinant of Down syndrome-related developmental cognitive deficits

Li Zhang[1,2], Kai Meng[2], Xiaoling Jiang[2], Chunhong Liu[2], Annie Pao[2], Pavel V. Belichenko[5], Alexander M. Kleschevnikov[5], Sheena Josselyn[6], Ping Liang[7], Ping Ye[8], William C. Mobley[5,*,†] and Y. Eugene Yu[2,3,4,*,†]

[1]Department of Physiology and Pathophysiology, Medical School of Xi'an Jiaotong University, Xi'an, Shaanxi, China, [2]The Children's Guild Foundation Down Syndrome Research Program, Genetics Program and Department of Cancer Genetics, Roswell Park Cancer Institute, Buffalo, NY 14263, USA, [3]New York State Center of Excellence in Bioinformatics and Life Sciences, Buffalo, NY 14263, USA, [4]Department of Cellular and Molecular Biology, Roswell Park Division of Graduate School, State University of New York at Buffalo, Buffalo, NY 14263, USA, [5]Department of Neurosciences, School of Medicine, University of California at San Diego, La Jolla 92093, CA, USA, [6]Neurosciences and Mental Health Program, Hospital for Sick Children, Toronto, ON, Canada M5G 1X8, [7]Department of Biological Sciences, Brock University, St Catharines, ON, Canada L2S 3A1 and [8]School of Molecular Biosciences, Washington State University, Pullman, WA 99164, USA

Received April 25, 2013; Revised July 29, 2013; Accepted September 11, 2013

Trisomy 21 (Down syndrome, DS) is the most common genetic cause of developmental cognitive deficits, and the so-called Down syndrome critical region (DSCR) has been proposed as a major determinant of this phenotype. The regions on human chromosome 21 (Hsa21) are syntenically conserved on mouse chromosome 10 (Mmu10), Mmu16 and Mmu17. DSCR is conserved between the *Cbr1* and *Fam3b* genes on Mmu16. Ts65Dn mice carry three copies of ~100 Hsa21 gene orthologs on Mmu16 and exhibited impairments in the Morris water maze and hippocampal long-term potentiation (LTP). Converting the *Cbr1-Fam3b* region back to two copies in Ts65Dn mice rescued these phenotypes. In this study, we performed similar conversion of the *Cbr1-Fam3b* region in *Dp(16)1Yey/+* mice that is triplicated for all ~115 Hsa21 gene orthologs on Mmu16, which also resulted in the restoration of the wild-type phenotypes in the Morris water maze and hippocampal LTP. However, converting the *Cbr1-Fam3b* region back to two copies in a complete model, *Dp(10)1Yey/+;Dp(16)1Yey/+;Dp(17)1Yey/+*, failed to yield the similar phenotypic restorations. But, surprisingly, converting both the *Cbr1-Fam3b* region and the Hsa21 orthologous region on Mmu17 back to two copies in the complete model did completely restore these phenotypes to the wild-type levels. Our results demonstrated that the Hsa21 orthologous region on Mmu17 is a major determinant of DS-related developmental cognitive deficits. Therefore, the inclusion of the three copies of this Hsa21 orthologous region in mouse models is necessary for unraveling the mechanism underlying DS-associated developmental cognitive deficits and for developing effective interventions for this clinical manifestation.

*To whom correspondence should be addressed. Fax: +1 7168451698 (Y.E.Y.)/+1 8585348980 (W.C.M.); Email: yuejin.yu@roswellpark.org (Y.E.Y.)/wmobley@ucsd.edu (W.C.M.)
†W.C.M. and Y.E.Y. contributed equally to this paper.

INTRODUCTION

The presence of an extra copy of human chromosome 21 (Hsa21), i.e. trisomy 21, causes Down syndrome (DS). Trisomy 21 is the most common human aneuploidy compatible with postnatal survival and the most common genetic cause of developmental cognitive deficits (1,2). The average IQ of people with DS is significantly lower when compared with people without DS. Substantial evidence has shown that hippocampal dysfunctions are associated with cognitive deficits in DS (2,3). But the precise underlying molecular mechanism is not well understood, and no effective treatments have been developed for this clinical condition.

To better understand DS and to develop future therapeutic interventions, the mouse has become the indispensable model organism for DS based on the evolutionary conservation between the human and mouse genomes. The regions on Hsa21 are syntenically conserved with three regions in the mouse genome located on mouse chromosome 10 (Mmu10), Mmu16 and Mmu17, which contain ∼41, 115 and 19 Hsa21 gene orthologs which encode protein or miRNA, respectively (Figs 1 and 4; http://www.ensembl.org; http://genome.ucsc.edu, last accessed date on 18 September 2013). The Ts65Dn strain is the first viable trisomic mouse model of DS, which is the chromosomally unbalanced progeny of a mouse mutant carrying a balanced translocation; the genetic alteration was randomly induced by irradiation at Muriel Davisson's laboratory (4,5). The unbalanced derivative chromosome in the mutant mice, i.e. Ts(17^{16})65Dn, consists of a genomic fragment of ∼13 Mb extending from *miR-155* to the telomere on Mmu16 with ∼51% of the Hsa21 orthologous region and ∼57% of the Hsa21 gene orthologs triplicated (Fig. 1) (6,7). Ts65Dn mice consistently exhibit impairments of hippocampal-mediated cognitive behaviors, including impairment in the Morris water maze test (5). At the neurophysiological level, impairment of hippocampal long-term potentiation (LTP) was also consistently observed in Ts65Dn mice (8,9). Recently, a mouse mutant carrying a duplication spanning the entire Hsa21 orthologous region

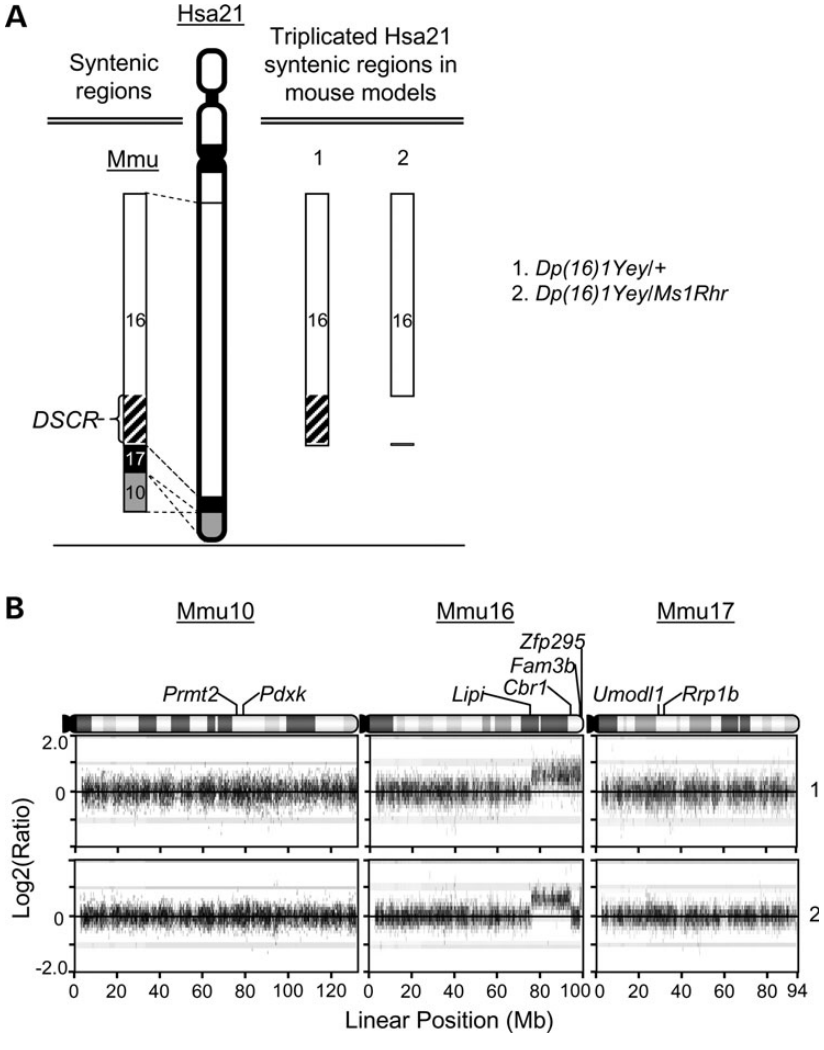

Figure 1. The mouse models of DS carrying three copies in the different Hsa21 orthologous regions on Mmu16. (**A**) Schematic representation of Hsa21 and the triplicated Hsa21 syntenic regions in the mouse models. (**B**) Agilent microarray CGH profiles show the duplication [*Dp(16)1Yey*] and the deletion [*Ms1Rhr*] in the Hsa21 orthologous region on Mmu16. CGH profiles 1 and 2 were generated using the DNA samples isolated from mouse models 1 and 2, respectively (A). No genomic alterations were detected on Mmu10 and Mmu17. Plotted are $\log_2$-transformed hybridization ratios of the DNA from mutants versus wild-type mouse DNA. The endpoint genes of the Hsa21 orthologous regions and the *Ms1Rhr* region are shown.

on Mmu16, *Dp(16)1Yey*/+, was developed using recombinase-mediated chromosome engineering (10). Similar to Ts65Dn mice, *Dp(16)1Yey*/+ mice also exhibit impairments in the hippocampal-mediated cognitive behaviors, such as impairment in the Morris water maze test, and hippocampal LTP (11). Subsequently, the mouse mutants carrying the duplications spanning the entire Hsa21 orthologous regions on Mmu10 and Mmu17, *Dp(10)1Yey*/+ and *Dp(17)1Yey*/+, respectively, were developed using chromosome engineering. Importantly, the compound mutant carrying all the three engineered duplications, i.e. *Dp(10)1Yey*/+;*Dp(16)1Yey*/+;*Dp(17)1Yey*/+, also exhibit impairments in the hippocampal-mediated cognitive behaviors, such as the Morris water maze test, and hippocampal LTP (12).

Segmental trisomies of Hsa21 have been used for genetic analysis of Hsa21 regions associated with a specific phenotype of DS (13–16). During these investigative efforts, the Down syndrome critical region (DSCR) was proposed as a critical genomic region on Hsa21 underlying major DS phenotypes, including developmental intellectual disabilities (17,18). *Ms1Rhr* mouse mutant was engineered carrying a deletion between *Cbr1* and *Fam3b* on Mmu16, the mouse orthologous region of the human DSCR (19). Ts65Dn/*Ms1Rhr* mice, the progeny from crossing Ts65Dn mice with *Ms1Rhr* mice, did not exhibit impairments in the cognitive behaviors, such as the Morris water maze test, and the hippocampal LTP (20). The result from this genetic subtractive experiment showed that the *Cbr1-Fam3b* region is required for the Ts(17^{16})65Dn chromosome to exert its impact on the cognitive phenotypes in Ts65Dn mice.

The aforementioned studies suggest a possibility that Ts65Dn, *Dp(16)1Yey*/+ and *Dp(10)1Yey*/+;*Dp(16)1Yey*/+;*Dp(17)1Yey*/+ mutants may share a similar mechanism underlying the hippocampal-associated phenotypes. In addition, the *Cbr1-Fam3b* region may be the only major genetic determinant of the DS-related developmental cognitive phenotypes, and other Hsa21 orthologous regions may play only minor roles in affecting the developmental cognitive phenotypes in DS. In this study, we set out to test these important possibilities by utilizing the mouse mutants configured specifically for the tasks.

RESULTS

The *Cbr1-Fam3b* region is necessary for the Hsa21 orthologous region on Mmu16 to cause DS-related learning and memory deficits

The so-called DSCR was proposed as a critical genomic region on Hsa21 responsible for the DS phenotypes, including developmental cognitive disability (17,18). In mice, the DSCR is conserved in the *Cbr1-Fam3b* region on Mmu16 (Fig. 1A). To examine the contribution of the *Cbr1-Fam3b* region to the impact of Mmu16-associated cognitive phenotypes in DS, we employed *Dp(16)1Yey*/+ and *Ms1Rhr* mice, which were engineered to carry the duplication spanning the entire Hsa21 orthologous region and the deletion of the *Cbr1-Fam3b* region on Mmu16, respectively (10,19). By crossing these mutants, we generated the progeny with the genotypes of *Dp(16)1Yey*/+, *Dp(16)1Yey/Ms1Rhr* (Fig. 1B) or +/+. The genomic contents of these two mouse models were analyzed by array-based comparative genomic hybridization (CGH), which shows the duplication in the Hsa21 orthologous region on Mmu16 in *Dp(16)1Yey*/+ mice and the *Cbr1-Fam3b* region was converted back to two copies in *Dp(16)1Yey/Ms1Rhr* mice (Fig. 1B). To examine the contribution of the *Cbr1-Fam3b* region to *Dp(16)1Yey*-associated impairment of hippocampal-mediated learning and memory, we compared the performances of these three groups of mice in the Morris water maze test. In the hidden platform version, although both latency and the path-length needed for the mice to locate the platform significantly decreased with training for all the mutant mice and the wild-type control mice ($P < 0.01$, Fig. 2A and B), there were significant differences in both latency ($F_{2,24} = 13.88$, $P < 0.01$, Fig. 2A) and the path length ($F_{2,24} = 11.02$, $P < 0.05$, Fig. 2B) needed for locating the platform among the three groups. *Dp(16)1Yey*/+ mice took a longer average latency and path length than *Dp(16)1Yey/Ms1Rhr* or +/+ mice, but there was no significant difference in latency and path length between *Dp(16)1Yey/Ms1Rhr* and wild-type control mice ($P > 0.05$, Fig. 2A and B). Because latency is affected by swimming speed, the path-length is a more definitive indicator. In the visible platform version, there was no statistically significant difference in the path-lengths ($F_{2,33} = 3.04$, $P > 0.05$) in locating the platform among these groups of the mice (Fig. 2B). In the probe test carried out on the day after the training trials, there was a significant difference in the time spent in the target quadrant (northeast, NE) among these groups ($F_{2,29} = 3.57$, $P < 0.05$, Fig. 2D). *Dp(16)1Yey*/+ mice spent a significantly shorter time in the target quadrant (NE) than the wild-type control mice ($P < 0.05$, Fig. 2D), but also shorter time than *Dp(16)1Yey/Ms1Rhr* mice ($P < 0.05$, Fig. 2D). Additional comparison shows no difference between *Dp(16)1Yey/Ms1Rhr* mice and the wild-type control mice in their time spent in the target quadrant ($P > 0.05$, Fig. 2D). These results showed that although *Dp(16)1Yey* causes impairment in the Morris water maze test, compounding it with *Ms1Rhr* led to the complete restoration of the performance of the mice in this test to the wild-type level. These results indicate that the presence of three copies of the *Cbr1-Fam3b* region is necessary for *Dp(16)1Yey* to exert its impact on the DS-related learning and memory deficits in mice.

The *Cbr1-Fam3b* region is necessary for the Hsa21 orthologous region on Mmu16 to cause DS-related impairment of hippocampal LTP

To explore the physiological basis of the performances of *Dp(16)1Yey*/+ and *Dp(16)1Yey/Ms1Rhr* mice in the Morris water maze test, we carried out *in vitro* analysis of hippocampal synaptic transmission and plasticity by utilizing electrophysiological recordings in the CA1 region of the hippocampus in brain slices. First, we assessed the basal synaptic transmission by analyzing field excitatory postsynaptic potentials (fEPSPs) evoked by stimuli of various intensities and found no significant difference in the input/output curve among the three groups of the mice ($F_{2,29} = 0.44, P > 0.05$, Fig. 3A). To examine presynaptic function, we compared paired-pulse facilitation and found neither *Dp(16)1Yey*/+ nor *Dp(16)1Yey/Ms1Rhr* genotype has significant effect on this short-lasting form of synaptic plasticity ($F_{2,29} = 0.46$, $P > 0.05$, Fig. 3B). We then investigated hippocampal LTP, which is considered a major physiological mechanism of learning and memory (21,22). LTP of the CA1 region of the hippocampus in brain slices was induced by theta-burst stimulation (TBS). Mean fEPSP slopes were measured for 60 min after

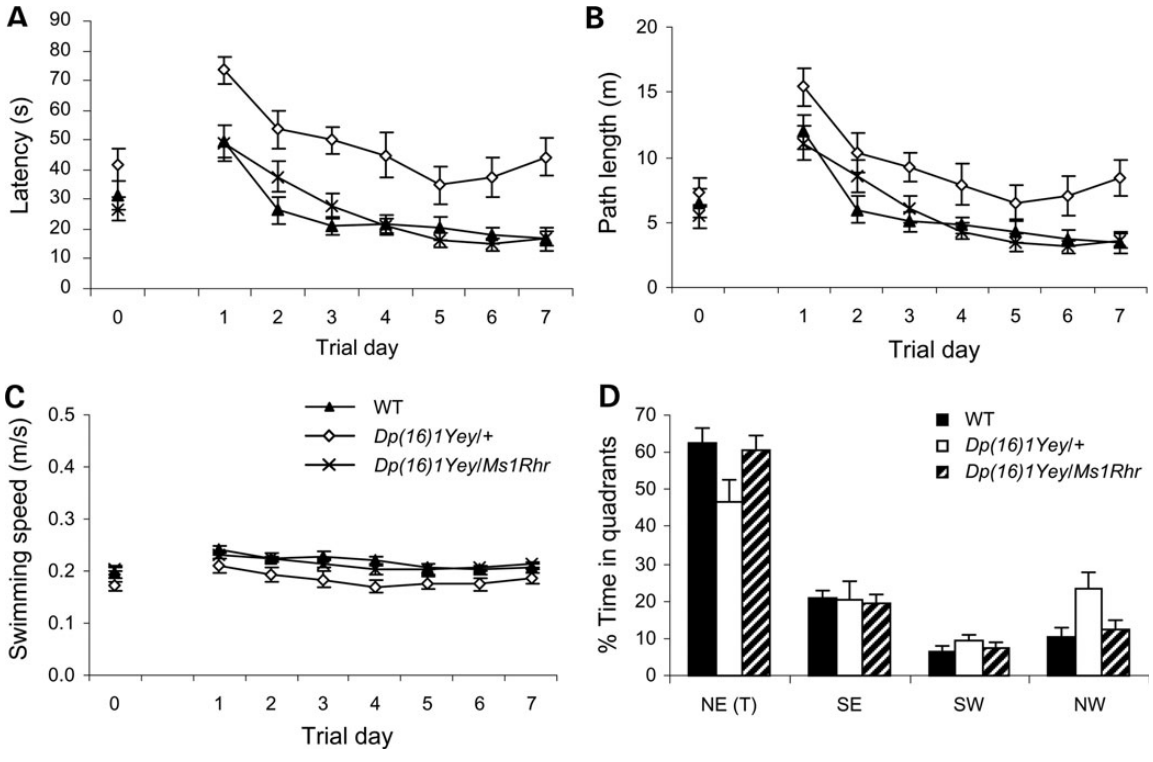

Figure 2. Analysis of the contribution of the *Cbr1-Fam3b* region to the Mmu16-associated performance in the Morris water maze test by the mouse models of DS. The *Dp(16)1Yey/+* ($n = 11$), *Dp(16)1Yey/Ms1Rhr* ($n = 10$) and the wild-type control mice ($n = 11$) were examined in the Morris water maze. (**A**) Latency to locate the platform (s). (**B**) Path-length to locate the platform (m). (**C**) Swimming speed (m/s). (**D**) The relative amount of time spent in different quadrants during the probe test 1 day after the end of the training trials.

TBS. There was a significant difference of the mean synaptic response after TBS among the three genotypes ($F_{2,29} = 14.65$, $P < 0.001$, Fig. 3C). The mean synaptic response after TBS of *Dp(16)1Yey/+* mice was significantly lower than that of the wild-type control mice ($P < 0.0001$, Fig. 3C) or *Dp(16)1Yey/Ms1Rhr* mice ($P < 0.001$, Fig. 3C). There was no difference in the mean synaptic response between the latter two ($P > 0.05$, Fig. 3C). Thus, these results showed that although *Dp(16)1Yey* causes impairment in hippocampal LTP, compounding it with *Ms1Rhr* led to completely restore the hippocampal LTP of the mice to the wild-type level, indicating that the presence of three copies of the *Cbr1-Fam3b* region is necessary for *Dp(16)1Yey* to exert its impact on hippocampal LTP in mice.

Hsa21 orthologous region on Mmu17 is a major determinant of DS-related learning and memory deficits in mice

Using the engineered chromosomal rearrangements *Dp(16)1Yey* and *Ms1Rhr*, we demonstrated above the absolute requirement of the *Cbr1-Fam3b* region in order for *Dp(16)1Yey* on Mmu16 to cause DS-related cognitive impairments (Figs 1–3). But Mmu16 is not the only mouse chromosome that harbors an Hsa21 orthologous region. Therefore, to accurately assess the impact of the *Cbr1-Fam3b* region on DS-related cognitive impairments in mice, we generated *Dp(10)1Yey/+;Dp(16)1Yey/Ms1Rhr;Dp(17)1Yey/+* and *Dp(10)1Yey/+;Dp(16)1Yey/+;Dp(17)1Yey/+* mice (Fig. 4). In order to assess the potential contributions of other Hsa21 orthologous regions to cognitive phenotypes in DS, we generated and characterized additional compound mutants beyond *Dp(10)1Yey/+;Dp(16)1Yey/+;Dp(17)1Yey/+* mice, *Dp(10)1Yey/+;Dp(16)1Yey/Ms1Rhr;Dp(17)1Yey/+* mice (Fig. 4) and the wild-type control mice. The genomic contents of these mouse models were analyzed by array-based CGH, which shows the triplication of different Hsa21 orthologous regions as the consequences of the different combinations of a duplication(s) and a deletion (Fig. 4B). In the hidden platform version of the Morris water maze test, although both latency and the path-length needed for mice to locate the platform significantly decreased with training for all the mutant mice and their wild-type control mice ($P < 0.0001$, Fig. 5A and B), there were significant differences in both latency ($F_{5,73} = 11.20$, $P < 0.0001$, Fig. 5A) and the path-length ($F_{5,73} = 8.55$, $P < 0.0001$, Fig. 5B) needed for locating the platform among the groups. Because the latency is affected by swimming speed, the path-length is a more definitive indicator. In the visible platform version, there was no statistically significant difference in the path-lengths ($F_{5,73} = 0.65$, $P > 0.05$, Fig. 5B) in locating the platform among these groups of the mice. A probe test was carried out on the day after the training trials when the platform was removed from the water. Based on the path-length and the time spent in the target quadrant, the mice can be divided into two groups [Group 1: +/+, *Dp(10)1Yey/+;Dp(16)1Yey/Ms1Rhr* and *Dp(10)1Yey/+;Dp(17)1Yey/+*. Group 2: *Dp(10)1Yey/+;Dp(16)1Yey/Ms1Rhr*; *Dp(17)1Yey/+*, *Dp(16)1Yey/Ms1Rhr;Dp(17)1Yey/+*, and *Dp(10)1Yey/+;Dp(16)1Yey/+;Dp(17)1Yey/+*]. The mice with the genotypes of Group 1 performed better in the Morris water maze than the mice with the genotypes of Group 2. The *post hoc* analysis showed there were differences in the path-length

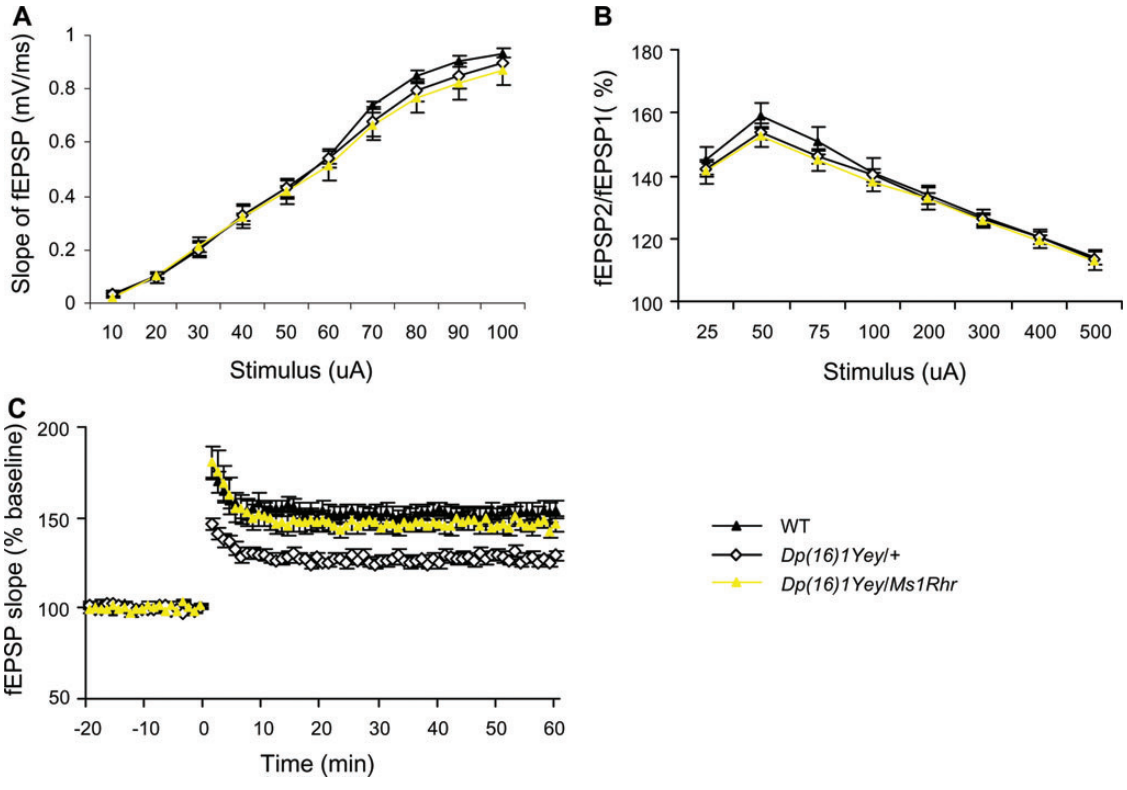

Figure 3. Analysis of the contribution of the *Cbr1-Fam3b* region to the Mmu16-associated electrophysiological phenotype in the mouse models of DS. *In vitro* characterizations of hippocampal synaptic transmission and plasticity were carried out by utilizing electrophysiological recordings in the CA1 region of the hippocampus in the brain slices of the *Dp(16)1Yey/+* mice ($n = 12$), *Dp(16)1Yey/Ms1Rhr* mice ($n = 10$) and the wild-type control mice ($n = 10$). (**A**) Input–output curves were generated by applying stimuli of increasing intensity and measuring the initial slopes of the fEPSPs. (**B**) Paired-pulse facilitation was measured by applying two closely spaced stimuli and was expressed as the ratio of synaptic responses (fEPSP2/fEPSP1) as a function of interstimulus interval. (**C**) For measuring hippocampal LTP, the fEPSPs were induced by TBS. Recordings were carried out before and after TBS inductions for the DS mouse models and the wild-type control mice. Evoked potentials were normalized to the fEPSP recorded prior to TBS induction (baseline = 100%). The data are presented as the percentage of fEPSP as a function of time.

and the time spent in the target quadrant between any genotypes from the two different groups ($P < 0.05$) but no difference in either of these two parameters between any genotypes within the same group ($P > 0.05$) (Fig. 5). The results from this experiment indicate that converting the *Cbr1-Fam3b* region from three to two copies in the triple-duplication model is not sufficient to restore hippocampal-mediated learning and memory to the wild-type level, and only simultaneous conversions of both the *Cbr1-Fam3b* region and the Hsa21 orthologous region on Mmu17 from three to two copies can rescue this phenotype.

Hsa21 orthologous region on Mmu17 is a major determinant of DS-related hippocampal LTP impairment in mice

To explore the physiological basis of the performances of the compound mutants in the Morris water maze test, we carried out *in vitro* analysis of hippocampal synaptic transmission and plasticity by utilizing electrophysiological recording in the CA1 region of the hippocampus in brain slices. First, we assessed the basal synaptic transmission by analyzing fEPSPs evoked by stimuli of various intensities and found no difference in the input/output curve among all the mutant groups and the wild-type control mice ($F_{5,59} = 0.22$, $P > 0.05$; Fig. 6A). To examine presynaptic function, we compared paired-pulse facilitation and found none of the mutant genotype has significant effect on this short-lasting form of synaptic plasticity ($F_{5,59} = 0.28$, $P > 0.05$, Fig. 6B). We then investigated LTP of the CA1 region of the hippocampus, which was induced by TBS. There was a significant difference of the mean synaptic response after TBS among the genotypes ($F_{5,59} = 14.80$, $P < 0.001$). The mean synaptic responses after TBS of *Dp(10)1Yey/+;Dp(16)1Yey/Ms1Rhr* and *Dp(10)1Yey/+;Dp(17)1Yey/+* mice appeared similar to those of the wild-type control mice ($P > 0.05$). The mean synaptic responses after TBS of *Dp(10)1Yey/+;Dp(16)1Yey/Ms1Rhr;Dp(17)1Yey/+* and *Dp(16)1Yey/Ms1Rhr;Dp(17)1Yey/+* mice were similar between these two genotypes ($P > 0.05$) but were significantly lower than those of wild-type control mice ($P < 0.05$). The mean synaptic response after TBS of *Dp(10)1Yey/+;Dp(16)1Yey/+;Dp(17)1Yey/+* mice was significantly lower than that of the mice with all other genotypes ($P < 0.05$) (Fig. 6C).

DISCUSSION

In this study, we analyzed the contributions of different Hsa21 orthologous regions to the DS-related developmental cognitive phenotypes in mice. The DSCR was proposed as a critical genomic region on Hsa21 responsible for the DS phenotypes, including developmental cognitive deficits (17,18). In mice, the DSCR is conserved in the *Cbr1-Fam3b* region on Mmu16. Converting the *Cbr1-Fam3b* region from three copies to two copies

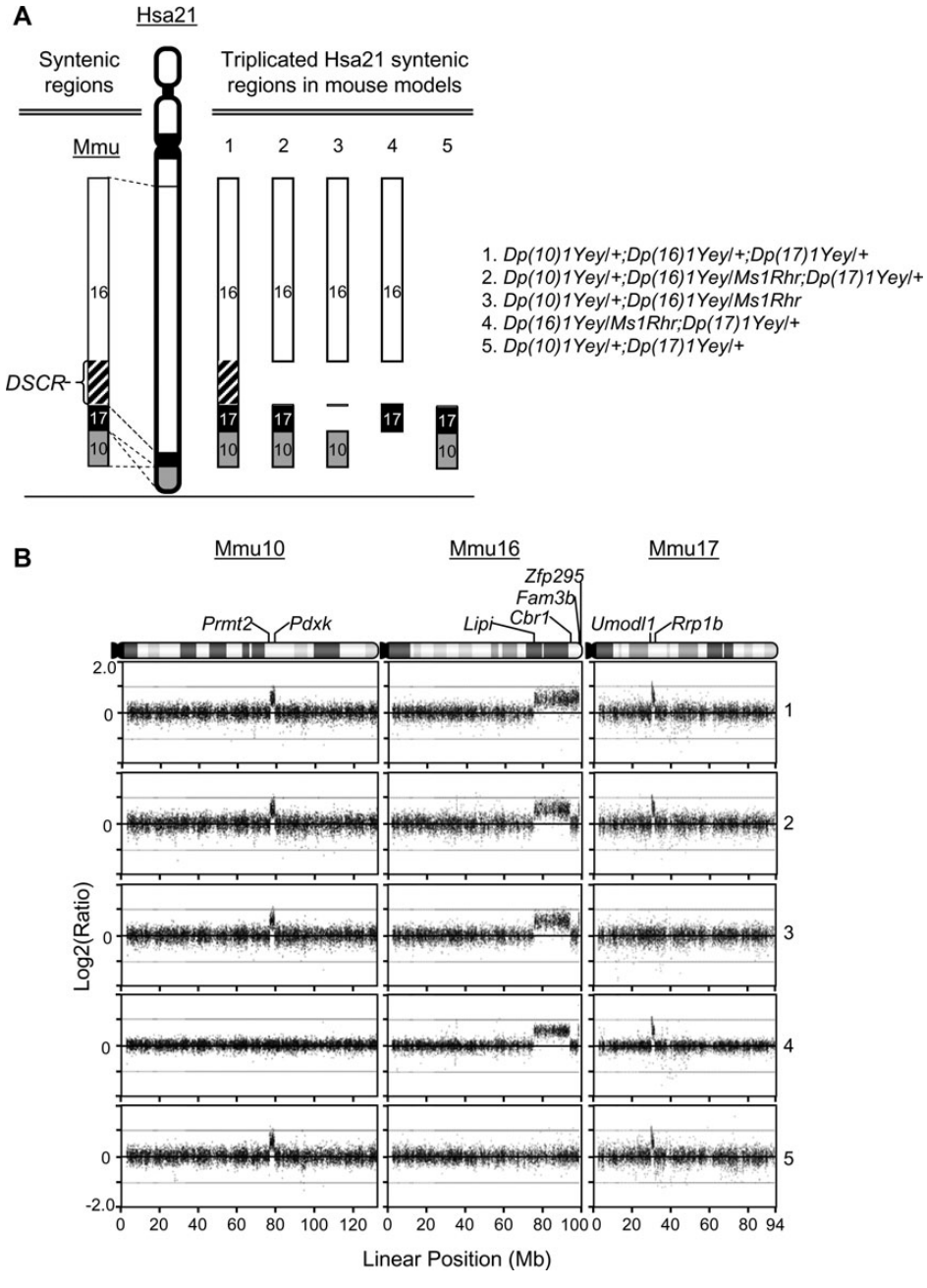

Figure 4. The mouse models of DS carrying three copies in the different Hsa21 orthologous regions on Mmu10, Mmu16 and Mmu17. (**A**) Schematic representation of Hsa21 and the triplicated Hsa21 syntenic regions in the mouse models. (**B**) Agilent microarray CGH profiles show duplications [*Dp(10)1Yey*, *Dp(16)1Yey* and *Dp(17)1Yey*] and the deletion [*Ms1Rhr*] in the Hsa21 orthologous region on Mmu10, Mmu16 and Mmu17. CGH profiles 1, 2, 3, 4 and 5 were generated using the DNA samples isolated from mouse models 1, 2, 3, 4 and 5, respectively (A). Plotted are $\log_2$-transformed hybridization ratios of the DNA from mutants versus wild-type mouse DNA. The endpoint genes of the Hsa21 orthologous regions and the *Ms1Rhr* region are shown.

in Ts65Dn mice completely rescued the cognitive phenotypes caused by the presence of the Ts(17^{16})65Dn chromosome, i.e. impairments shown in the Morris water maze test and in hippocampal LTP measurement (20). However, Ts65Dn mice cannot be used to conclusively assess the contribution of the *Cbr1-Fam3b* region to Mmu16-associated cognitive phenotypes for the following reasons: first, the entire Hsa21 orthologous region on Mmu16 spans from *Lipi* to *Zfp295* and contains ∼15 more Hsa21 gene orthologs than the Ts(17^{16})65Dn chromosome (http://www.ensembl.org, last accessed date on 18 September 2013) (6,7); second, Ts65Dn mice also carry a trisomic segment of an ∼10 Mb subcentromeric region on Mmu17 that is not syntenic to a region on Hsa21, and this trisomic region contains ∼60 protein- and miRNA-coding genes (6,7). Because *Dp(16)1Yey/+* mice carry the duplication spanning the entire Hsa21 orthologous region on Mmu16, the complete rescue of impairments in the Morris water maze test and hippocampal LTP by *Ms1Rhr* in the compound mutant *Dp(16)1Yey/Ms1Rhr* indicates that the *Cbr1-Fam3b* region is absolutely necessary for the Hsa21 orthologous region on Mmu16 to exert its impact

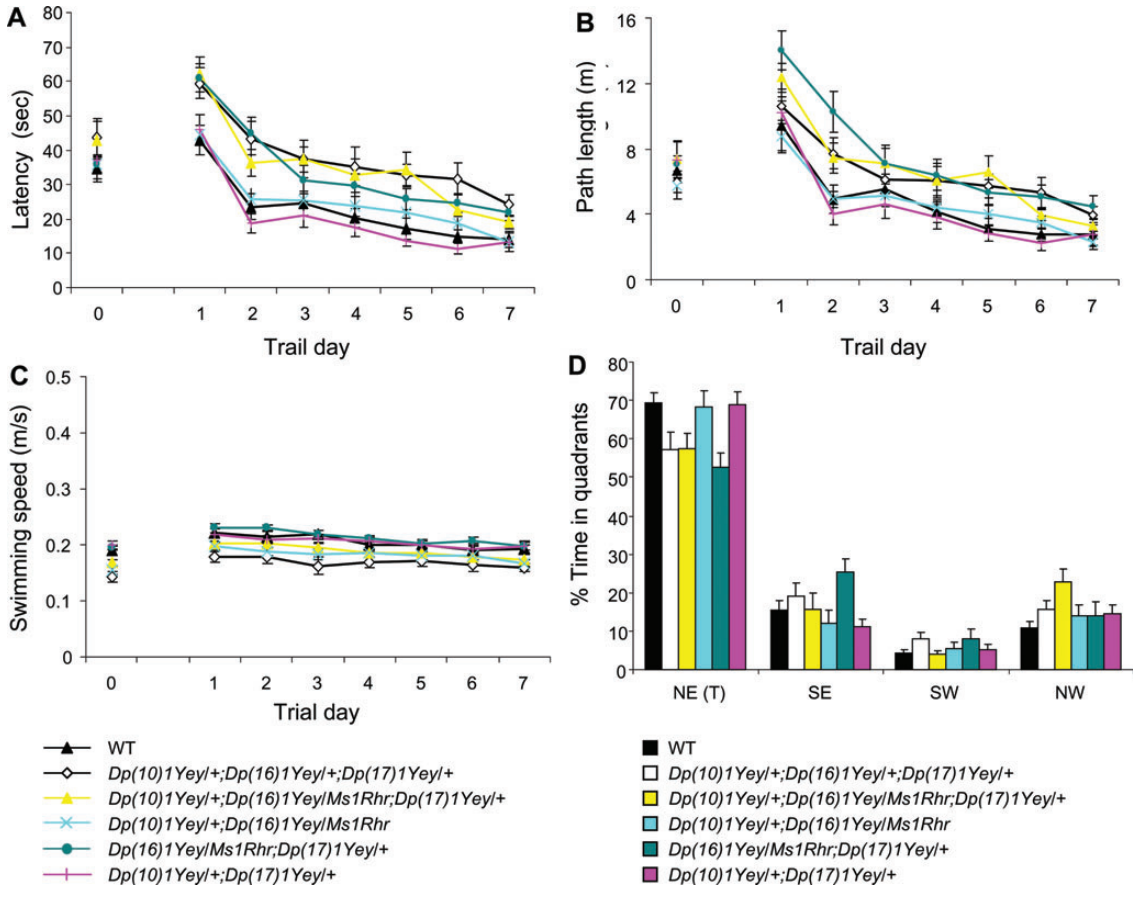

Figure 5. Analysis of the contributions of the *Cbr1-Fam3b* region and the Hsa21 orthologous region on Mmu17 to the performance in the Morris water maze test by the mouse models of DS. The *Dp(10)1Yey/+;Dp(16)1Yey/+;Dp(17)1Yey/+* ($n = 12$), *Dp(10)1Yey/+;Dp(16)1Yey/Ms1Rhr;Dp(17)1Yey/+* ($n = 14$), *Dp(10)1Yey/+;Dp(16)1Yey/Ms1Rhr* ($n = 13$), *Dp(16)1Yey/Ms1Rhr;Dp(17)1Yey/+* ($n = 14$), *Dp(10)1Yey/+;Dp(17)1Yey/+* ($n = 13$) and the wild-type control mice ($n = 13$) were examined in the Morris water maze. (**A**) Latency to locate the platform (s). (**B**) Path-length to locate the platform (m). (**C**) Swimming speed (m/s). (**D**) The relative amount of time spent in different quadrants during the probe test 1 day after the end of the training trials.

on DS-related cognitive deficits. This result supports the possibility that Ts65Dn and *Dp(16)1Yey/+* mice may share the similar mechanism underlying the phenotypes.

With its essential role established using *Dp(16)1Yey/Ms1Rhr* mice, we explored the impact of the *Cbr1-Fam3b* region in a complete genetic model. Surprisingly, we found that converting the *Cbr1-Fam3b* region from three copies to two copies in the complete genetic model did not significantly improve the cognitive performance in the Morris water maze test, made evident by the data from the *Dp(10)1Yey/+;Dp(16)1Yey/+;Dp(17)1Yey/+* and *Dp(10)1Yey/+;Dp(16)1Yey/Ms1Rhr;Dp(17)1Yey/+* mice (Fig. 5). This observation was supported by the results from the electrophysiology experiments in which the hippocampal LTP in *Dp(10)1Yey/+;Dp(16)1Yey/Ms1Rhr;Dp(17)1Yey/+* mice remains significantly impaired when compared with that of the +/+ mice, although there is an improvement when compared with the hippocampal LTP in the *Dp(10)1Yey/+;Dp(16)1Yey/+;Dp(17)1Yey/+* mice. Another surprise from this study is the detrimental effect of the segmental trisomies completely disappeared when both the *Cbr1-Fam3b* region and the Hsa21 orthologous region on Mmu17 were converted from three copies to two copies. This result indicated that, among the Hsa21 orthologous regions, the orthologous region on Mmu17 plays a determining role in causing DS-related cognitive deficits. Our result support the data generated by Julie Korenberg's laboratory using patients carrying segmental trisomies of Hsa21 (13).

Interestingly, the drastic adverse impact of the Mmu17-associated Hsa21 orthologous region on the cognitive phenotypes is revealed only by the analysis of the compound mutants. When *Dp(17)1Yey/+* mice were examined, we detected only a small increase in hippocampal LTP but no impairment in the Morris water maze test (11) (Li *et al.*, unpublished data). The phenotypes are similar between *Dp(10)1Yey/+;Dp(16)1Yey/Ms1Rhr;Dp(17)1Yey/+* and *Dp(16)1Yey/Ms1Rhr;Dp(17)1Yey/+* mice, indicating that the impact of the Hsa21 orthologous regions on Mmu17 is the consequence of the interaction between *Dp(17)1Yey* and the other duplicated region(s) on Mmu16 located outside the *Cbr1-Fam3b* region (Fig. 4).

Our results demonstrated that, for DS-related developmental cognitive deficits, the DSCR is not the sole determinant and the Hsa21 orthologous region on Mmu17 also plays a decisive role, so understanding how the latter affects the phenotypic outcome may be essential to unravel the underlying molecular mechanism. For the same reason, the contribution of the Hsa21 orthologous region on Mmu17 will need to be included in any animal models to be used for developing effective therapeutic

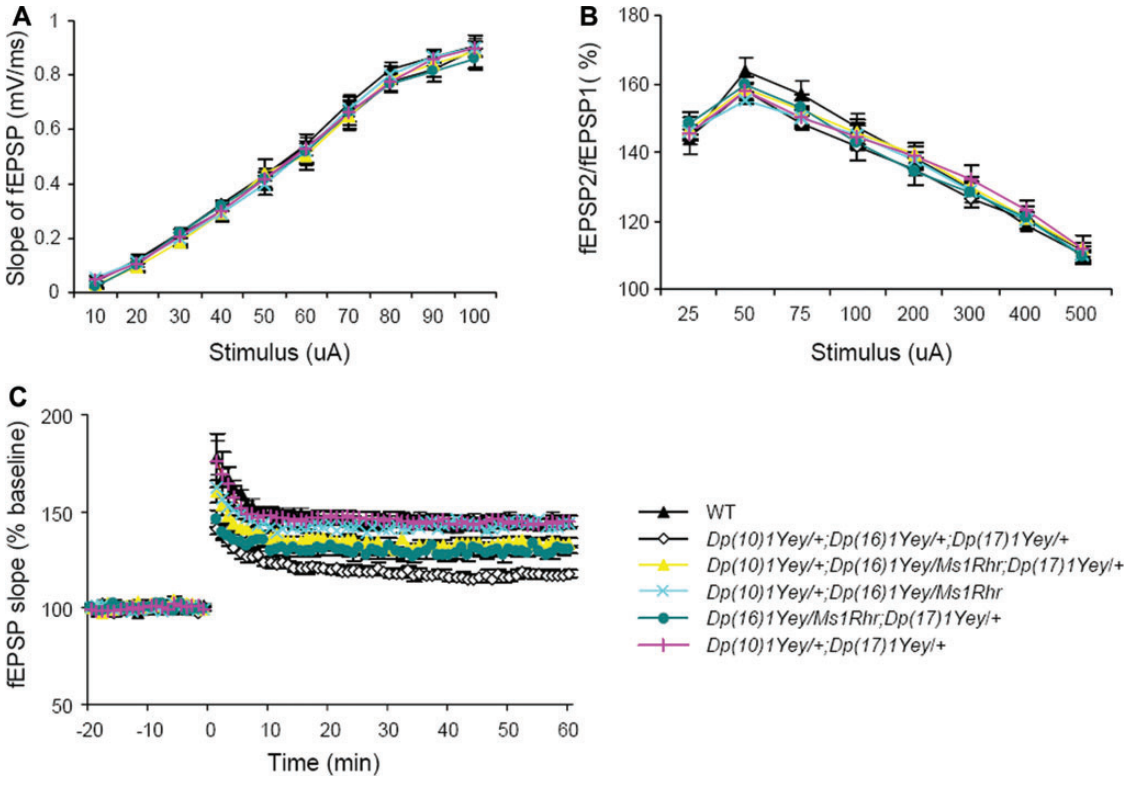

Figure 6. Analysis of the contributions of the *Cbr1-Fam3b* region and the Hsa21 orthologous region on Mmu17 to the electrophysiological phenotype in the mouse models of DS. *In vitro* characterizations of hippocampal synaptic transmission and plasticity were carried out by utilizing electrophysiological recordings in the CA1 region of the hippocampus in the brain slices of the *Dp(10)1Yey/+;Dp(16)1Yey/+;Dp(17)1Yey/+* ($n = 12$), *Dp(10)1Yey/+;Dp(16)1Yey/Ms1Rhr;Dp(17)1Yey/+* ($n = 11$), *Dp(10)1Yey/+;Dp(16)1Yey/Ms1Rhr* ($n = 10$), *Dp(16)1Yey/Ms1Rhr;Dp(17)1Yey/+* ($n = 10$), *Dp(10)1Yey/+;Dp(17)1Yey/+* ($n = 10$) and the wild-type control mice ($n = 12$). (**A**) Input–output curves were generated by applying stimuli of increasing intensity and measuring the initial slopes of the fEPSPs. (**B**) Paired-pulse facilitation was measured by applying two closely spaced stimuli and was expressed as the ratio of synaptic responses (fEPSP2/fEPSP1) as a function of the interstimulus interval. (**C**) For measuring hippocampal LTP, the fEPSPs were induced by TBS. Recordings were carried out before and after TBS inductions for the DS mouse models and the wild-type control mice. Evoked potentials were normalized to the fEPSP recorded prior to TBS induction (baseline = 100%). The data are presented as the percentage of fEPSP as a function of time.

interventions. Ts65Dn mice have been used extensively for developing therapeutic interventions, including pharmacological agents, for treating cognitive deficits in individuals with DS (23–28). Based on our results, it is therefore possible that the therapeutic interventions effective for enhancing cognitive function in Ts65Dn mice may not have the similar effect in patients with DS because the Hsa21 orthologous region on Mmu17 is not present in three copies in Ts65Dn mice (29).

Our current analysis of the mutants carrying different combinations of the duplication(s) and deletion has revealed the critical Hsa21 orthologous regions underlying developmental cognitive deficits in DS. Potential candidate genes which may be causally associated with the phenotypes we observed could be selected from these genomic regions based on their functions. For instance, *Dyrk1a* and *Kcnj6* in the *Cbr1-Fam3b* region on Mmu16 and *Pde9a* in the Hsa21 orthologous region on Mmu17 have been predicted as the critical dosage-sensitive genes for developmental cognitive deficits (30,31). *Dyrk1a* encodes a dual-specificity tyrosine-phosphorylation-regulated kinase which has been shown to play an important role in signaling transduction in biological processes, including those in the central nervous system (32–34). DYRK1A may contribute to a phenotype through the regulating activity of the nuclear factor of activated T-cells (35). *Kcnj6* encodes a G-protein-activated potassium channel, which regulates neuronal excitability by mediating inhibitory effects of G-protein-coupled receptors for neuromodulators and neurotransmitters (36,37). Triplication of *Kcnj6* in Ts65Dn mice resulted in an increase in the G-protein-activated potassium channel (38) and may thereby alter the inhibitory tone of the synapses. Introducing a heterozygous null allele of *Kcnj6* into Ts65Dn mice led to a decrease in the resting membrane potential of CA1 pyramidal neurons (39), but the direct impact of *Kcnj6* on hippocampal LTP remains unknown. *Pde9a* expresses in the hippocampus. The enzyme PDE9A, encoded by this gene, is a negative regulator in glutamatergic signaling and memory formation by degrading cGMP to 5′GMP (40–42). An extra copy of *PDE9A* in individuals with DS may abnormally reduce glutamate signaling, thereby causing impairment in memory formation. For the Hsa21 orthologous region proximal to the *Cbr1-Fam3b* region on Mmu16, *C21orf62* has recently been implicated in intellectual disability (http://www.genome.gov/27551936, last accessed date on 18 September 2013). The contributions of these candidate genes to the phenotypes we observed could be examined by a 'subtractive strategy'. *Dyrk1a* and *Kcnj6* could be analyzed in *Dp(16)1Yey/Dyrk1a−* and *Dp(16)1Yey/Kcnj6−* mutants, respectively. To examine the impact of both these genes simultaneously,

one of the null alleles could be transferred to the *Dp(16)1Yey* chromosome through meiotic crossover. Assessing the contribution of *Pde9a* and *C21orf62* to the phenotypes we observed will be more complex because of the interaction of the genomic regions where these two genes are located. Each gene will need to be examined in a model with triplications of the interacting genomic regions, such as the *Dp(16)1Yey/Ms1Rhr;Dp(17)1Yey/+* model, using the subtractive strategy. Therefore, *Pde9a* and *C21orf62* could be analyzed in the *Dp(16)1/Ms1Rhr;Dp(17)1Yey/Pde9a−* mutant and the *Dp(16)1Yey/C21orf62-;Ms1Rhr;Dp(17)1Yey/+* mutant, respectively. To generate the latter, the *Ms1Rhr* deletion will first need to be transferred to the *Dp(16)1Yey* chromosome via meiotic crossover.

Although the above approach is feasible for assessing the impacts of individual potential candidate genes on the mutant phenotypes, it is not the most efficient strategy to identify the causal genes. This is because the Hsa21 orthologous regions associated with the phenotypes we observed contain 134 Hsa21 gene orthologs, and the potential contributions of the vast majority of these genes to the mutant phenotypes cannot be excluded. Therefore, in order to identify the critical gene(s) using the above approach, it may need to examine most of these 134 genes one by one. Alternative to this direct candidate gene screening approach which requires an enormous amount of effort, a far more efficient strategy starts with generating and analyzing desirable new duplications and deletions in the Hsa21 orthologous regions to unbiasedly narrow down the critical genomic regions. It has been previously shown that the duplication of the *Cbr1-Fam3b* region is sufficient to cause cognitive deficits in the Ts1Rhr mice (30), and in this study we showed that the duplication of the *Cbr1-Fam3b* region is necessary to cause cognitive deficits in *Dp(16)1Yey/+* mice (Figs 2 and 3). Therefore, this genomic region can be dissected independently, which contains 30 protein-coding Hsa21 gene orthologs but no miRNA-coding gene ortholog. Because the *Kcnj15* gene is located in the middle of the region, *Cbr1-Kcnj15* and *Kcnj15-Fam3b* segments will divide the genomic region into two with a similar number of protein-coding genes in each region. Generating and analyzing *Ts1Rhr/Df(Cbr1-Kcnj15)* mice (19) can reveal whether the *Cbr1-Kcnj15* region contains a critical gene(s) whose triplication is necessary to cause a mutant phenotype. Generating and analyzing *Dp(Cbr1-Kcnj15)/+* mice can reveal whether the same genomic region contains the critical gene(s) whose triplication is sufficient to cause the mutant phenotype. This combination of strategies using a duplication alone and in combination with a smaller deletion could also be utilized to analyze the *Kcnj15-Fam3b* region as well as the sub-regions in order to narrow down the critical genomic regions. After a minimal critical region(s) is established through systematic genetic mapping, a causal gene can be identified by generating and analyzing a compound mutant which carries a duplication of the minimal critical region and a null allele of a candidate gene located within the region. A similar strategy can be used to identify the critical Hsa21 gene orthologs located proximal to the *Cbr1-Fam3b* region on Mmu16. However, owing to the regional interaction observed in this study, the presence of *Dp(17)1Yey* in the testing models will be necessary in order to dissect the Hsa21 orthologous region proximal to the *Cbr1-Fam3b* region on Mmu16 using the aforementioned strategy. Likewise, to dissect Hsa21 orthologous region on Mmu17, the presence of *Dp(16)1Yey/Ms1Rhr* in the testing models will be necessary.

The molecular genetic mechanism underlying DS-related developmental cognitive deficits may be complex, but our success in establishing the role of the Hsa21 orthologous region on Mmu17 shows the power of mouse mutants carrying defined duplications and deletions in molecular genetic dissection of DS. Future expansion of this type of efforts should greatly facilitate the mechanistic studies as well as the endeavors to develop novel interventional strategies.

MATERIALS AND METHODS

Animals

Dp(10)1Yey/+, *Dp(16)1Yey/+* and *Dp(17)Yey/+* mice, developed using recombinase-mediated chromosome engineering, carry duplications spanning the entire Hsa21 orthologous regions on Mmu10, Mmu16 and Mmu17, respectively (10,11). Individual duplication strains were backcrossed to C57BL/6J mice for five generations. These duplication mice were maintained by sibling mating with the wild-type littermates. *Ms1Rhr* [*Del(16Cbr1-ORF9)1Rhr*] mice were obtained from the Jackson Laboratory. *Ms1Rhr* mice were crossed with *Dp(16)1Yey/+* to generate *Dp(16)1Yey/Ms1Rhr* mice and the compound mutant mice were then backcrossed with *Dp(16)1Yey/+* mice for four generations. Afterwards, *Dp(16)1Yey/Ms1Rhr* and *Dp(16)1Yey/+* mice from this backcross were bred with *Dp(16)1Yey/+* mice and the wild-type littermates from our *Dp(16)1Yey/+* colony, respectively. The progeny from these mating experiments, *Dp(16)1Yey/Ms1Rhr*, *Dp(16)1Yey/+* and *+/+* mice, were used in the experiments for examining the contribution of the *Cbr1-Fam3b* region to Mmu16-associated cognitive phenotypes in DS. In the experiments for examining the contributions of different Hsa21 orthologous regions on Mmu10, Mmu16 and Mmu17, including the *Cbr1-Fam3b* region, to DS-related cognitive phenotypes, we first crossed the individual duplication strains to generate *Dp(10)1Yey/+;Dp(16)1Yey/+;Dp(17)1Yey/+* mice and then crossed the triple duplication mice with *Dp(16)1/Ms1Rhr* or *+/+* mice generated from the previous set of the experiment. The progeny with the following genotypes were used in the phenotyping experiments: *Dp(10)1Yey/+;Dp(16)1Yey/+;Dp(17)1Yey/+*, *Dp(10)1Yey/+;Dp(16)1Yey/Ms1Rhr;Dp(17)1Yey/+*, *Dp(10)1Yey/+;Dp(16)1/Ms1Rhr*, *Dp(16)1Yey/Ms1Rhr;Dp(17)1Yey/+*, *Dp(10)1Yey/+;Dp(17)1Yey/+* and *+/+*. The genotypes of the mutants were determined as described previously (10,11) (http://jaxmice.jax.org/protocolsdb/f?P=116:2:948584393376459::NO:2:P2_MASTER_PROTOCOL_ID,P2_JRS_CODE:1503,005654).

The mutant mice and the wild-type control mice were maintained in a 12 h light and dark schedule with *ad libitum* access to food and water and a temperature- and humidity-controlled animal facility. All mice used in the experiments were 2–4 months old. Before behavioral experiments, each mouse was pre-handled for 2 min every day for a week. The experimental procedures were approved by the Institutional Animal Care and Use Committee at the Roswell Park Cancer Institute.

Array-based CGH

The genomic content of each mouse model was analyzed by array-based CGH (12). An oligonucleotide array containing 180 000 probes designed for mouse CGH was utilized (SurePrint G3 Mouse CGH Microarray Kit, 4 × 180K; Agilent Technologies, Inc.), which is composed of 60-mer oligonucleotides. The array provides comprehensive coverage of the mouse genome, and the genome coordinates of the probes in the array were predetermined by Agilent Technologies. Genomic DNA was prepared from the tail tissue using the DNeasy Tissue Kit (Qiagen, Inc., Valencia, CA, USA). Genomic DNA samples isolated from wild-type littermates were used as reference controls. For mutants *Dp(16)1Yey/+*, *Dp(10)1Yey/+;Dp(16)1Yey/+;Dp(17)1Yey/+*, *Dp(10)1Yey/+;Dp(16)1Yey/Ms1Rhr;Dp(17)1Yey/+*, *Dp(10)1Yey/+;Dp(16)1Yey/Ms1Rhr* and *Dp(10)1Yey/+;Dp(17)1Yey/+*, the genomic DNA samples were isolated from female mice; so, the genomic DNAs from the wild-type male littermates were used as reference controls. For mutants *Dp(16)1Yey/Ms1Rhr* and *Dp(16)1Yey/Ms1Rhr;Dp(17)1/+*, the genomic DNA samples were isolated from male mice; so, the genomic DNA from the wild-type female littermates was used as the reference control. The genomic DNA samples from the mouse mutants and the wild-type littermates (1 μg each) were fluorescently labeled using the Agilent Genomic DNA Labeling Kit. Hybridization to the Agilent mouse 180K CGH array was performed for 40 h at 65°C. After hybridization, the slides were washed and scanned in an Agilent microarray scanner to generate high-resolution images for both Cy3 (the mutant mice) and Cy5 (the wild-type littermates) channels. Image analysis was performed using Agilent Genomic Workbench 7.0 (Agilent Technologies, Inc.).

Morris water maze test

A standard Morris water maze test was carried out in a circular pool (152 cm in diameter) of water at 25 ± 1°C (12). The experimental data were collected and analyzed using HVS Water 2020, an imaging-tracking and analysis system (HVS Image Ltd, Twickenham, Middlesex, UK). Visible-platform training trials were carried out on day 1 and each mouse had four trials. The distance traveled (path-length) in finding the platform was recorded. The hidden-platform training trials were carried out on days 2–8 and each mouse had four trials each day. The amount of time spent in finding the platform (latency), the distance traveled (path-length) and the swimming speed were recorded. On day 9, a probe test was performed in which the platform was removed from the water and each mouse was allowed 60 s to search the pool. Times spent in different quadrants were recorded.

Hippocampal slice preparation

The procedures for electrophysiological recordings were described previously (8,43). Briefly, after the brains were removed from the mice, they were placed in an ice-cold solution bubbled with 95% O_2–5% CO_2 (pH 7.4), which comprised the following (in mM): sucrose 110, NaCl 60, KCl 3, NaH_2PO_4 1.25, $NaHCO_3$ 28, $MgSO_4$ 7, (+)-sodium-L-ascorbate 0.6, $CaCl_2$ 0.5 and glucose 5. The hippocampal formation was resected, and the middle third portion was cut into 350 μm-thick transverse slices using a vibratome. The slices were transferred to an interface recording chamber (Automate Scientific, Inc., CA, USA) and submerged in the artificial cerebrospinal fluid, which comprised the following (in mM): NaCl 119, KCl 3.5, $NaHCO_3$ 26.2, $MgSO_4$ 1.3, NaH_2PO_4 1, $CaCl_2$ 2.5 and glucose 11. The chamber was maintained at a constant temperature (28 ± 1°C) and the slices were allowed to equilibrate for at least 1 h. The upper surfaces of the slices were in contact with a humidified and oxygenated (95% O_2–5% CO_2) stream.

Electrophysiological recordings and induction of synaptic plasticity

Standard extracellular recording techniques were employed (8,43). Schaffer collateral-commissural fibers were stimulated with a bipolar Teflon-coated tungsten electrode (Microprobes, MD, USA). Extracellular fEPSPs were recorded using a glass microelectrode filled with 2 M NaCl (2–3 MΩ) positioned in the stratum radiatum of the CA1 hippocampal area. For baseline recordings, 0.1 ms test stimuli were delivered once per 20 s (0.05 Hz) for at least 20 min to ensure response stabilization. Basal synaptic transmission was examined based on the relationship between the stimulus intensity and the initial fEPSP slope (i.e. input–output curve). Based on this input–output relationship, the stimulation intensity was set to yield 50–60% maximal response for the rest of the electrophysiological experiments for each genotype. Paired-pulse facilitation, a short-lasting form of synaptic plasticity indicative of presynaptic release probability, was assessed by measuring two closely spaced synaptic responses (fEPSP2/fEPSP1) at various interstimulus intervals. For LTP measurement, TBS was applied after 20 min of stable baseline recording. TBS included 15 trains at 5 Hz, with each train consisting of four pulses at 100 Hz. Signals from recording electrodes were amplified with a microelectrode AC amplifier (Model 1800; A-M Systems, WA, USA) and digitized into a computer file at a 10 kHz-sampling rate by using the Axon Digidata 1400A Data Acquisition System (Molecular Devices, Sunnyvale, CA, USA). Traces were obtained by pClamp 10.2 and analyzed using the Clampfit 10.2 program (Molecular Devices).

Data analysis

The data related to the hidden platform training trails of the Morris water maze tests, input–output curves and paired-pulse facilitation of electrophysiological experiments were subjected to repeated-measure analysis between genotypes, and *post hoc* analysis was performed using Fisher's LSD test. The data related to the visible platform training trials of the Morris water maze tests and probe tests and hippocampal LTP of electrophysiological experiments were subjected to a one-way ANOVA between genotypes, and *post hoc* analysis was carried out with a significance level of $P < 0.05$. In the electrophysiological analysis, *n* indicates the number of slices analyzed. In the behavioral phenotyping experiments, *n* indicates the number of mice.

ACKNOWLEDGEMENTS

Y.E.Y. would like to thank Dr Julie Korenberg for the insightful discussion on the importance of the Hsa21 orthologous region on Mmu17.

Conflict of Interest statement. None declared.

FUNDING

This project was supported in part by grants from the Children's Guild Foundation and the NIH (R01NS66072, R01HL91519 and P30CA16056).

REFERENCES

1. Pennington, B.F., Moon, J., Edgin, J., Stedron, J. and Nadel, L. (2003) The neuropsychology of Down syndrome: evidence for hippocampal dysfunction. *Child Dev.*, **74**, 75–93.
2. Pulsifer, M.B. (1996) The neuropsychology of mental retardation. *J. Int. Neuropsychol. Soc.*, **2**, 159–176.
3. Chapman, R.S. and Hesketh, L.J. (2000) Behavioral phenotype of individuals with Down syndrome. *Ment. Retard. Dev. Disabil. Res. Rev.*, **6**, 84–95.
4. Davisson, M.T., Schmidt, C. and Akeson, E.C. (1990) Segmental trisomy of murine chromosome 16: a new model system for studying Down syndrome. *Prog. Clin. Biol. Res.*, **360**, 263–280.
5. Reeves, R.H., Irving, N.G., Moran, T.H., Wohn, A., Kitt, C., Sisodia, S.S., Schmidt, C., Bronson, R.T. and Davisson, M.T. (1995) A mouse model for Down syndrome exhibits learning and behaviour deficits. *Nat. Genet.*, **11**, 177–184.
6. Duchon, A., Raveau, M., Chevalier, C., Nalesso, V., Sharp, A.J. and Herault, Y. (2011) Identification of the translocation breakpoints in the Ts65Dn and Ts1Cje mouse lines: relevance for modeling Down syndrome. *Mamm. Genome*, **22**, 674–684.
7. Reinholdt, L.G., Ding, Y., Gilbert, G.J., Czechanski, A., Solzak, J.P., Roper, R.J., Johnson, M.T., Donahue, L.R., Lutz, C. and Davisson, M.T. (2011) Molecular characterization of the translocation breakpoints in the Down syndrome mouse model Ts65Dn. *Mamm. Genome*, **22**, 685–691.
8. Kleschevnikov, A.M., Belichenko, P.V., Villar, A.J., Epstein, C.J., Malenka, R.C. and Mobley, W.C. (2004) Hippocampal long-term potentiation suppressed by increased inhibition in the Ts65Dn mouse, a genetic model of Down syndrome. *J. Neurosci.*, **24**, 8153–8160.
9. Siarey, R.J., Stoll, J., Rapoport, S.I. and Galdzicki, Z. (1997) Altered long-term potentiation in the young and old Ts65Dn mouse, a model for Down syndrome. *Neuropharmacology*, **36**, 1549–1554.
10. Li, Z., Yu, T., Morishima, M., Pao, A., LaDuca, J., Conroy, J., Nowak, N., Matsui, S., Shiraishi, I. and Yu, Y. (2007) Duplication of the entire 22.9-Mb human chromosome 21 syntenic region on mouse chromosome 16 causes cardiovascular and gastrointestinal abnormalities. *Hum. Mol. Genet.*, **16**, 1359–1366.
11. Yu, T., Liu, C., Belichenko, P., Clapcote, S.J., Li, S., Pao, A., Kleschevnikov, A., Bechard, A.R., Asrar, S., Chen, R. *et al.* (2010) Effects of individual segmental trisomies of human chromosome 21 syntenic regions on hippocampal long-term potentiation and cognitive behaviors in mice. *Brain Res.*, **1366**, 162–171.
12. Yu, T., Li, Z., Jia, Z., Clapcote, S.J., Liu, C., Li, S., Asrar, S., Pao, A., Chen, R., Fan, N. *et al.* (2010) A mouse model of Down syndrome trisomic for all human chromosome 21 syntenic regions. *Hum. Mol. Genet.*, **19**, 2780–2791.
13. Korbel, J.O., Tirosh-Wagner, T., Urban, A.E., Chen, X.N., Kasowski, M., Dai, L., Grubert, F., Erdman, C., Gao, M.C., Lange, K. *et al.* (2009) The genetic architecture of Down syndrome phenotypes revealed by high-resolution analysis of human segmental trisomies. *Proc. Natl Acad. Sci. USA*, **106**, 12031–12036.
14. Korenberg, J.R., Chen, X.N., Schipper, R., Sun, Z., Gonsky, R., Gerwehr, S., Carpenter, N., Daumer, C., Dignan, P. and Disteche, C. (1994) Down syndrome phenotypes: the consequences of chromosomal imbalance. *Proc. Natl Acad. Sci. USA*, **91**, 4997–5001.
15. Lyle, R., Bena, F., Gagos, S., Gehrig, C., Lopez, G., Schinzel, A., Lespinasse, J., Bottani, A., Dahoun, S., Taine, L. *et al.* (2009) Genotype-phenotype correlations in Down syndrome identified by array CGH in 30 cases of partial trisomy and partial monosomy chromosome 21. *Eur. J. Hum. Genet.*, **17**, 454–466.
16. Sinet, P.M., Theophile, D., Rahmani, Z., Chettouh, Z., Blouin, J.L., Prieur, M., Noel, B. and Delabar, J.M. (1994) Mapping of the Down syndrome phenotype on chromosome 21 at the molecular level. *Biomed. Pharmacother.*, **48**, 247–252.
17. Delabar, J.M., Theophile, D., Rahmani, Z., Chettouh, Z., Blouin, J.L., Prieur, M., Noel, B. and Sinet, P.M. (1993) Molecular mapping of twenty-four features of Down syndrome on chromosome 21. *Eur. J. Hum. Genet.*, **1**, 114–124.
18. Korenberg, J.R., Kawashima, H., Pulst, S.M., Ikeuchi, T., Ogasawara, N., Yamamoto, K., Schonberg, S.A., West, R., Allen, L., Magenis, E. *et al.* (1990) Molecular definition of a region of chromosome 21 that causes features of the Down syndrome phenotype. *Am. J. Hum. Genet.*, **47**, 236–246.
19. Olson, L.E., Richtsmeier, J.T., Leszl, J. and Reeves, R.H. (2004) A chromosome 21 critical region does not cause specific Down syndrome phenotypes. *Science*, **306**, 687–690.
20. Olson, L.E., Roper, R.J., Sengstaken, C.L., Peterson, E.A., Aquino, V., Galdzicki, Z., Siarey, R., Pletnikov, M., Moran, T.H. and Reeves, R.H. (2007) Trisomy for the Down syndrome 'critical region' is necessary but not sufficient for brain phenotypes of trisomic mice. *Hum. Mol. Genet.*, **16**, 774–782.
21. Bliss, T.V. and Collingridge, G.L. (1993) A synaptic model of memory: long-term potentiation in the hippocampus. *Nature*, **361**, 31–39.
22. Malenka, R.C. and Nicoll, R.A. (1999) Long-term potentiation—a decade of progress? *Science*, **285**, 1870–1874.
23. Braudeau, J., Delatour, B., Duchon, A., Pereira, P.L., Dauphinot, L., de Chaumont, F., Olivo-Marin, J.C., Dodd, R.H., Herault, Y. and Potier, M.C. (2011) Specific targeting of the GABA-A receptor alpha5 subtype by a selective inverse agonist restores cognitive deficits in Down syndrome mice. *J. Psychopharmacol.*, **25**, 1030–1042.
24. Contestabile, A., Greco, B., Ghezzi, D., Tucci, V., Benfenati, F. and Gasparini, L. (2013) Lithium rescues synaptic plasticity and memory in Down syndrome mice. *J. Clin. Invest.*, **123**, 348–361.
25. Fernandez, F., Morishita, W., Zuniga, E., Nguyen, J., Blank, M., Malenka, R.C. and Garner, C.C. (2007) Pharmacotherapy for cognitive impairment in a mouse model of Down syndrome. *Nat. Neurosci.*, **10**, 411–413.
26. Gardiner, K.J. (2010) Molecular basis of pharmacotherapies for cognition in Down syndrome. *Trends Pharmacol. Sci.*, **31**, 66–73.
27. Kleschevnikov, A.M., Belichenko, P.V., Faizi, M., Jacobs, L.F., Htun, K., Shamloo, M. and Mobley, W.C. (2012) Deficits in cognition and synaptic plasticity in a mouse model of Down syndrome ameliorated by GABAB receptor antagonists. *J. Neurosci.*, **32**, 9217–9227.
28. Martinez-Cue, C., Martinez, P., Rueda, N., Vidal, R., Garcia, S., Vidal, V., Corrales, A., Montero, J.A., Pazos, A., Florez, J. *et al.* (2013) Reducing GABAA alpha5 receptor-mediated inhibition rescues functional and neuromorphological deficits in a mouse model of Down syndrome. *J. Neurosci.*, **33**, 3953–3966.
29. Hanney, M., Prasher, V., Williams, N., Jones, E.L., Aarsland, D., Corbett, A., Lawrence, D., Yu, L.M., Tyrer, S., Francis, P.T. *et al.* (2012) Memantine for dementia in adults older than 40 years with Down's syndrome (MEADOWS): a randomised, double-blind, placebo-controlled trial. *Lancet*, **379**, 528–536.
30. Belichenko, N.P., Belichenko, P.V., Kleschevnikov, A.M., Salehi, A., Reeves, R.H. and Mobley, W.C. (2009) The 'Down syndrome critical region' is sufficient in the mouse model to confer behavioral, neurophysiological, and synaptic phenotypes characteristic of Down syndrome. *J. Neurosci.*, **29**, 5938–5948.
31. Pereira, P.L., Magnol, L., Sahun, I., Brault, V., Duchon, A., Prandini, P., Gruart, A., Bizot, J.C., Chadefaux-Vekemans, B., Deutsch, S. *et al.* (2009) A new mouse model for the trisomy of the Abcg1-U2af1 region reveals the complexity of the combinatorial genetic code of Down syndrome. *Hum. Mol. Genet.*, **18**, 4756–4769.
32. Hammerle, B., Ulin, E., Guimera, J., Becker, W., Guillemot, F. and Tejedor, F.J. (2011) Transient expression of Mnb/Dyrk1a couples cell cycle exit and differentiation of neuronal precursors by inducing p27KIP1 expression and suppressing NOTCH signaling. *Development*, **138**, 2543–2554.

33. Fernandez-Martinez, J., Vela, E.M., Tora-Ponsioen, M., Ocana, O.H., Nieto, M.A. and Galceran, J. (2009) Attenuation of Notch signalling by the Down-syndrome-associated kinase DYRK1A. *J. Cell Sci.*, **122**, 1574–1583.
34. Kelly, P.A. and Rahmani, Z. (2005) DYRK1A enhances the mitogen-activated protein kinase cascade in PC12 cells by forming a complex with Ras, B-Raf, and MEK1. *Mol. Biol. Cell*, **16**, 3562–3573.
35. Gwack, Y., Sharma, S., Nardone, J., Tanasa, B., Iuga, A., Srikanth, S., Okamura, H., Bolton, D., Feske, S., Hogan, P.G. *et al.* (2006) A genome-wide *Drosophila* RNAi screen identifies DYRK-family kinases as regulators of NFAT. *Nature*, **441**, 646–650.
36. Mark, M.D. and Herlitze, S. (2000) G-protein mediated gating of inward-rectifier K+ channels. *Eur. J. Biochem.*, **267**, 5830–5836.
37. Yamada, M., Inanobe, A. and Kurachi, Y. (1998) G protein regulation of potassium ion channels. *Pharmacol. Rev.*, **50**, 723–760.
38. Harashima, C., Jacobowitz, D.M., Stoffel, M., Chakrabarti, L., Haydar, T.F., Siarey, R.J. and Galdzicki, Z. (2006) Elevated expression of the G-protein-activated inwardly rectifying potassium channel 2 (GIRK2) in cerebellar unipolar brush cells of a Down syndrome mouse model. *Cell. Mol. Neurobiol.*, **26**, 719–734.
39. Cramer, N.P., Best, T.K., Stoffel, M., Siarey, R.J. and Galdzicki, Z. (2010) GABAB-GIRK2-mediated signaling in Down syndrome. *Adv. Pharmacol.*, **58**, 397–426.
40. Domek-Lopacinska, K. and Strosznajder, J.B. (2005) Cyclic GMP metabolism and its role in brain physiology. *J. Physiol. Pharmacol.*, **56**(Suppl. 2), 15–34.
41. Domek-Lopacinska, K.U. and Strosznajder, J.B. (2010) Cyclic GMP and nitric oxide synthase in aging and Alzheimer's disease. *Mol. Neurobiol.*, **41**, 129–137.
42. Reneerkens, O.A., Rutten, K., Steinbusch, H.W., Blokland, A. and Prickaerts, J. (2009) Selective phosphodiesterase inhibitors: a promising target for cognition enhancement. *Psychopharmacology (Berl.)*, **202**, 419–443.
43. Zhang, L., Meng, K., Li, Y.H. and Han, T.Z. (2009) NR2A-containing NMDA receptors are required for L-LTP induction and depotentiation in CA1 region of hippocampal slices. *Eur. J. Neurosci.*, **29**, 2137–2144.